Available online at www.sciencedirect.com
SCIENCE DIRECT®
Engineering Geology 80 (2005) 199–213
ENGINEERING GEOLOGY
www.elsevier.com/locate/enggeo

Spatial risk analysis of Li-shan landslide in Taiwan

Keh-Jian Shou*, Ying-Liang Chen

Department of Civil Engineering, National Chung-Hsing University, 250 Kuo-Kuang Road, Taichung 402, Taiwan

Received 25 May 2004; received in revised form 21 April 2005; accepted 12 May 2005
Available online 16 June 2005

Abstract

By coupling limit equilibrium analysis and Monte Carlo analysis with a geography information system (GIS), this study implements a method that can evaluate the risk (corresponding to probability of failure in this study) of landslide with consideration of spatial uncertainties. The GIS can adopt the three-dimensional information including surface topography, underground geomaterial distribution and groundwater level to determine slope profiles for analysis. Then the safety of defined slope can be evaluated by limit equilibrium analysis. In this study, the mechanical properties of geomaterial were considered as random variables instead of single values. The slope and groundwater profiles are also randomly adopted. Through a Monte Carlo sampling process, a distribution of safety factor and probability of failure can be determined. This probabilistic risk analysis approach was applied to Li-shan landslide in Central Taiwan.

Due to heavy rains, the sites near the highway 7A (mileage 73 k+150) and the highway 8 (mileage 82 k) in the Li-shan Township began to subside in mid April 1990. Topography, geology, and groundwater condition of this area were first reviewed. Based on this review, together with field investigations and a series of limit equilibrium back analyses, a general hypothetic model was established to illustrate the failure mechanism of this landslide area. Then the developed probabilistic risk analysis model is applied to spatially evaluate the risk of this landslide area as well as the performance of the remediation treatment.

Keywords: Li-shan landslide; Risk estimation; Spatial uncertainty; Monte Carlo analysis; GIS; Probabilistic model

1. Introduction

Located at the midway of the east–west cross-island highway (the highway 8), Li-shan is an important small town not only for transportation but also for tourism in central Taiwan (see Fig. 1). In mid April 1990, due to heavy rain, the sites near the highway 7A (mileage 73 km+150 m) and the highway 8 (mileage 82 km) began to subside, as their foundations are located on one of the major sliding blocks in Li-shan landslide area. It is generally suggested that the Li-shan landslide is predominantly triggered by heavy rain together with the poor drainage condition.

* Corresponding author. Tel.: +886 4 22850989.
E-mail address: kjshou@dragon.nchu.edu.tw (K.-J. Shou).

0013-7952/$ - see front matter
doi:10.1016/j.enggeo.2005.05.002

Fig. 1. A bird eye view of the Li-shan landslide area (looking to the southwest).

To keep the highway open and the town secure for living, the government had executed the first phase emergency treatment followed by the second remediation treatment since July 1990. A drainage system including surface ditches, drainage wells and two drainage galleries was constructed and completed in early 2003. And the effectiveness of the remediation treatment has been strongly revealed as the Li-shan landslide survived the Chi-Chi earthquake (M_L=7.3) in 1999.

In view of the characteristics of the landslide area, it is of great interest to understand the complicated failure mechanism and spatially estimate the risk, which motivates this study. In this study, literatures about the topography, geology, and groundwater condition of this area were first reviewed. Based on this review, together with field investigations and a series of limit equilibrium back analyses, a general hypothetic model was established to primitively depict the failure mechanism of this landslide area. Then a probabilistic analysis approach is applied to spatially evaluate the risk of this landslide area.

As the stability analysis in geotechnical engineering can be biased due to the uncertainty of the input data, the probabilistic analysis approach (Chowdhury, 1982; Hoek, 1994; Juang et al., 1998; Shou and Wang, 2003) provides a better alternative. Geographic Information System (GIS) has strong capability in spatial data processing and geostatistical analysis. Therefore, it is useful and popular for the assessment of natural disasters. In this study, coupling limit equilibrium analysis and Monte Carlo analysis with a GIS, a probabilistic analysis approach was implemented to evaluate the risk of landslide with consideration of spatial uncertainties. Through this Monte Carlo type analysis, the risk of a slope can be evaluated by its probability of failure. This approach was applied to spatially evaluate the risk of Li-shan landslide.

2. Li-shan landslide

2.1. Geology

In western Taiwan, the westward thrust front due to the compression of the Philippine Sea Plate is obstructed by the rigid basement Peikang High (part of the Eurasian Plate). And this tectonic activity results in a series of Quaternary thrust faults trending north south and dipping towards the east (Ho, 1982; Lu et al., 2000). The Li-shan fault, a major ridge fault of the Taiwan Island is also generated by this tectonic activity. It is located less than 3 kilometers west of the Li-shan landslide (see Fig. 2). As Li-shan area is not far from the Li-shan fault, the geological condition in this area is more complicated than expected (Huang, 2002; Shou, 2002).

The Li-shan area is located in colluvial formations originally from the Miocene Lushan slate formation. Due to dynamic tectonic activities as well as the high precipitation, the surfacial slate formations in this area are highly weathered; it is strongly supported by the occurrence of slaty cleavages, foliation shears, and interlayers of silty residual soil. The testing results show that the Lushan unweathered slate is about 2.76 ton/m^3 of unit weight. The mechanical properties of the geomaterials with different weathered conditions are summarized in Table 1.

The annual precipitation in this area ranges from 1400 to 2200 mm with a concentration during May and September. Topographically, as being located at the western rim of Hsueh-shan ridge, Li-shan area dips toward the northwest and down to Tachia River with slope angle 15° to 30°.

2.2. Failure mechanism

The landslide area is about 76 hectares in size, and can be divided into three regions, i.e. the west, northeast, and southeast regions. And there are 7 to 20 sliding bodies in each region (see Fig. 3). Except the

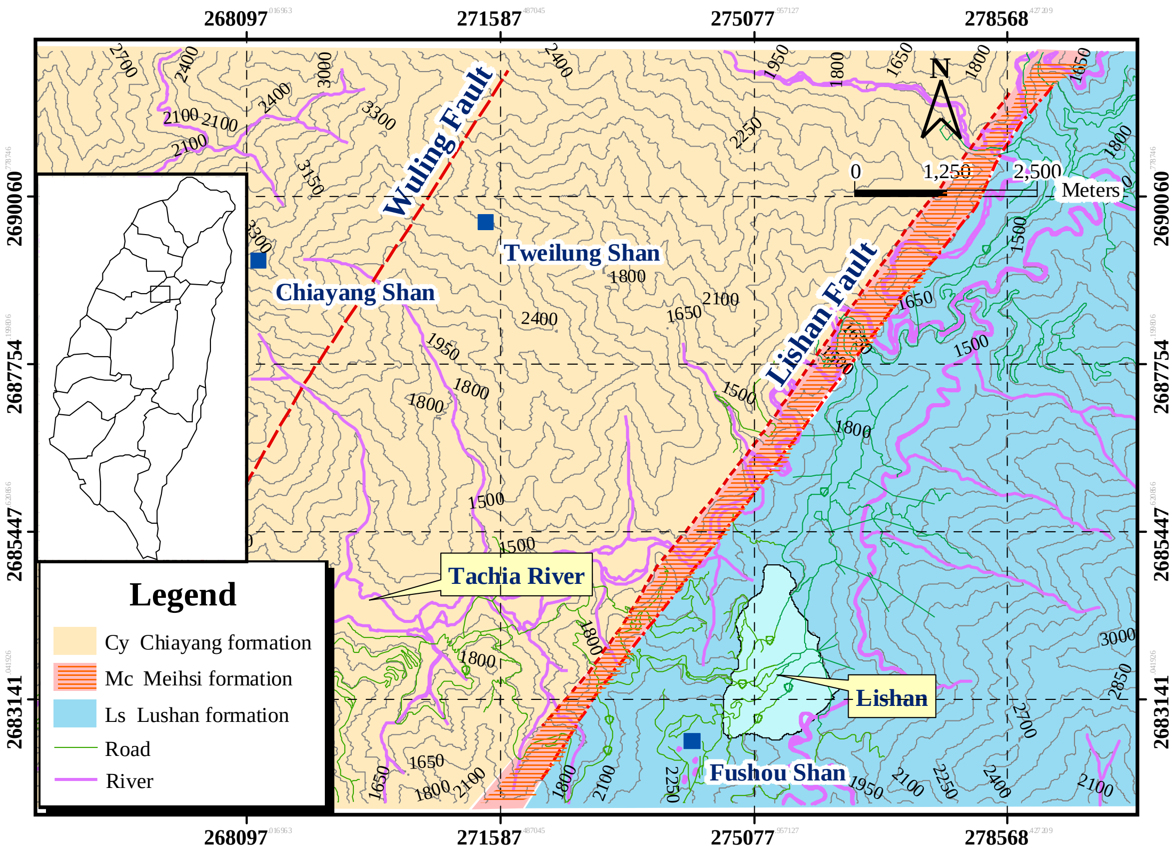

Fig. 2. Geologic map showing regional geology near Li-shan area. Li-shan landslide is mapped in the Miocene Lushan formation and Li-shan Fault is less than 3 km to the west.

southeast region, most of the unstable sliding bodies possess shallow sliding planes about 9–26 m below surface (Energy and Resources Laboratories, ITRI, 1993; Shou, 2002; Shou and Su, 2002). However, there is an old landslide near the profile BB′ within the southeast region, and the old sliding plane is more than 40–60 m below surface, according to the core logs and records of drainage gallery construction. And the rest of the southeast region is more or less located at the valley of a small branch of Tachia River. Due to the tectonic activities, there is rejuvenation activity in the Tachia River and the incision is accelerated (see Fig. 4). Therefore, the erosion rate of this branch is quite high, which provokes higher hazard potential of this sub region.

Based on the field investigations together with the topographical and geological information, a general hypothetic model was established to depict the Li-shan landslide. This model comprises major factors as: (1) the sliding planes is basically along the lower boundary of the regolith, about 20 m below the surface; (2) there is a major old landslide at the center of the landslide area; (3) the high erosion rate makes the slopes by the streams more unstable than the others.

Table 1
Mechanical properties of the geomaterial in Li-shan area

Geomaterial type	Unit weight (ton/m^3)	Cohesion c (ton/m^2)	Friction angle φ (°)
Colluvium	2.06	0.75	30
Medium to highly weathered slate	2.69	3.00	28
Fresh to medium weathered slate	2.76	30.00	33
Sliding plane	2.69	3.00	28

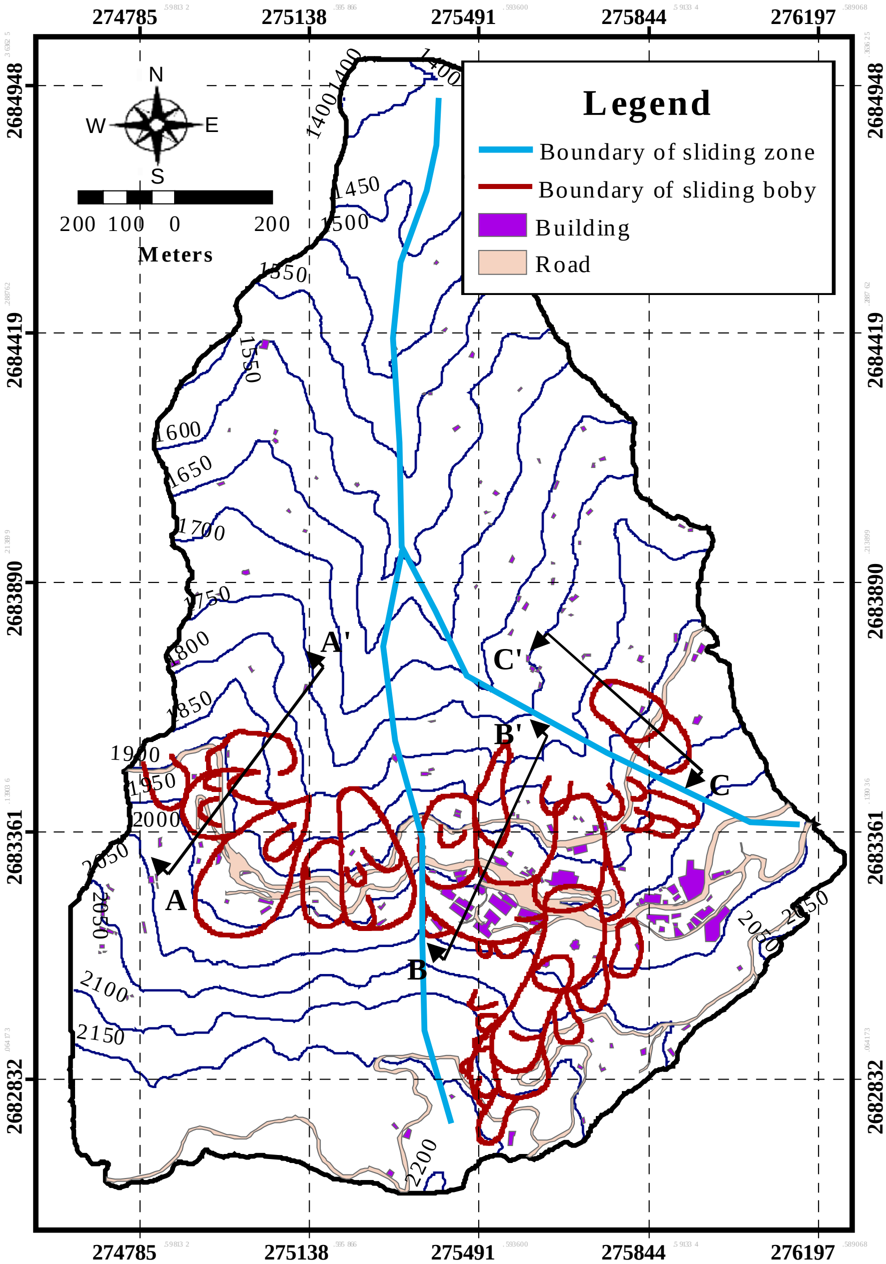

Fig. 3. Topography and division of Li-shan landslide area. More than 30 sliding bodies are distributed in three regions, i.e. west, southeast and northeast regions. Profiles AA′, BB′, and CC′ are adopted for preliminary stability back analysis.

Through a review of topography and major sliding bodies, the representative profiles AA′, BB′ and CC′ (see Fig. 3) were adopted for stability back analyses. The cross sections were determined based on the data from drilling. And the most critical sliding plane was considered in case of overlapping of sliding bodies. The back analyses were performed by the limit equilibrium analysis model PC-STABL6 (Bandini and

Salgado, 1999). The results show that those slopes are fairly stable for dry condition as the safety factor is 1.21–1.35. However, they become critical with high groundwater level as the safety factor drops to 0.99–1.15. This finding might reveal that there is more than one activity in this area, as the precipitation is quite high in this area (see Table 2).

2.3. Remediation

As the landslide is closely related with the rainfall and groundwater, groundwater control is essential for slope stabilization in this area. A drainage system, composed of surface and subsurface sub systems, was designed as a remediation treatment. For the surface drainage sub system, existing ditches were integrated as a system to divert the surface water to non-problem area, as well as to prevent excessive water infiltration near tension cracks. In order to more efficiently control the groundwater level, a subsurface drainage sub system is also applied, which is consisted of three major components, i.e., horizontal drainage pipe, drainage well, and drainage gallery. There are (1) 15 horizontal drainage sites, 7–9 pipes (30–60 m in length) in each site, (2) 13 drainage wells, located mainly in the heads of slopes, and (3) 2 drainage galleries, excavated below the sliding planes. The components of the drainage systems are illustrated in Fig. 5.

From the results of groundwater level monitoring, the groundwater level has been successfully reduced about 10–20 m after the drainage galleries in operation. By this improvement, the stability of slopes is reasonably improved as the safety factors are increased from 0.99–1.15 to 1.18–1.23 (see Table 2). Besides, during the Chi-Chi earthquake, the horizontal acceleration was estimated 0.15–0.20 g, and the groundwater level was raised no more than 1 m. With this impact, this area survived except minor damages near the profile BB′. It somehow reveals the effectiveness of the remediation.

Table 2
Safety factors of the residual slopes in Li-shan landslide

Profile analyzed	A-A′	B-B′	C-C′
Dry (no groundwater)	1.23	1.21	1.35
Wet (high groundwater level)	1.11	0.99	1.15
Wet (with remediation)	1.23	1.18	1.22

Fig. 4. The rejuvenation in the Tachia river makes the toe steeper than the head.

3. Methodology of analysis

3.1. GIS-probabilistic model

As Nguyen (1985) pointed out that a slope with a safety factor 2.5 is not twice as safe as that with a safety factor 1.25, and it is not necessary a slope with safety factor 1.5 more stable than a slope with safety factor 1.4. The safety factor itself might not be a complete index to illustrate the safety of a slope. The reason for that is the uncertainty behind the calculation of safety factor, including the variability of geomaterial properties as well as the uncertainties due to the sampling error, insufficient data, etc. One alternative way to treat the uncertainty is the probabilistic analysis approach.

With its power and versatility for processing spatial data, the Geographic Information System (GIS) is commonly applied for the assessment of natural disasters. GIS provides strong functions in database processing and geostatistical analysis. Therefore, it can be integrated with other analytical models, such as GIS-probabilistic infinite slope model (Pack et al., 1998; Zhou et al., 2003), GIS-infinite slope probabilistic seismic landslide model (Jibson et al., 1999; Khazai and Sistar, 2000), etc.

In this study, a GIS-probabilistic analysis approach was developed. Mechanical properties of geomaterial are considered as random variables instead of single

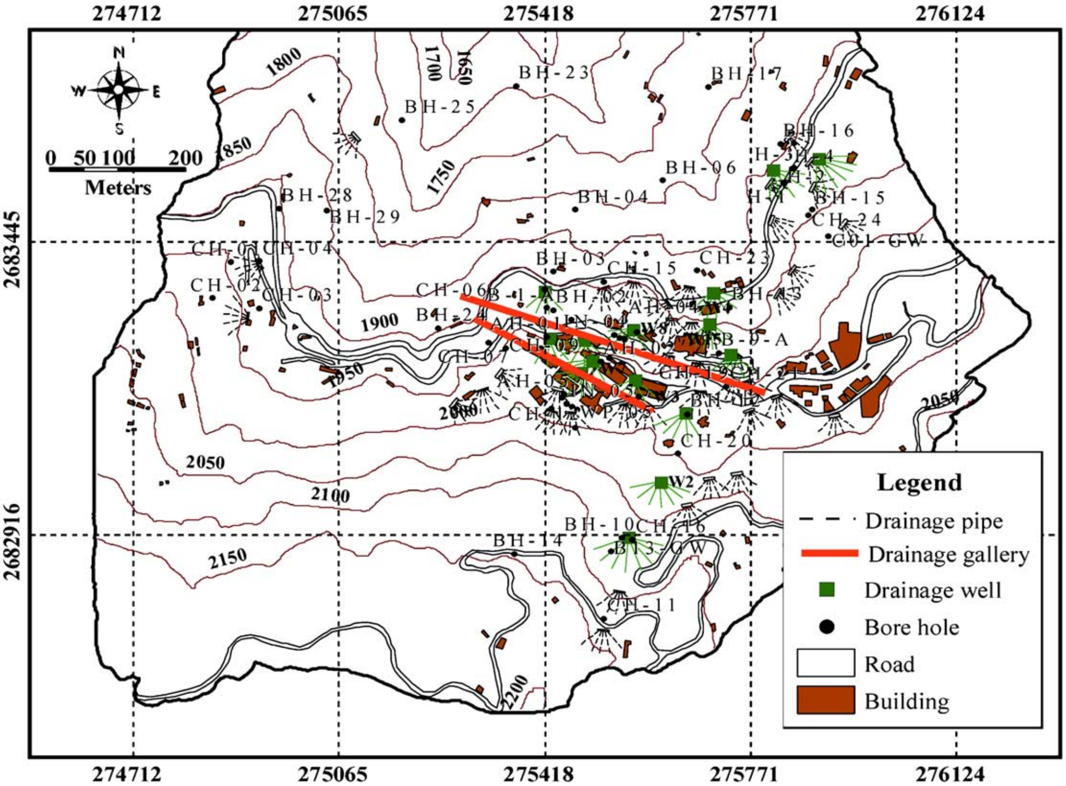

Fig. 5. The drainage system designed for remediation treatment.

values. And Monte Carlo sampling method is coupled with a GIS and limit equilibrium analysis method. Within the GIS, a Kriging process is applied to determine the three-dimensional elevation model as well as the slope profiles for stability analysis.

To estimate a value at a point in a spatial domain with known observation data, Kriging is considered as a very powerful tool. Theoretically, it is a Best Linear Unbiased Estimator (Cressie, 1988). In this study, a Kriging process is used to get three-dimensional elevation model of rock depth and groundwater depth. The data from drilling and monitoring were stored and processed (kriged) by the GIS software with application of its spatial analysis modules.

As underground geology and groundwater conditions are quite different in those three regions, Kriging estimation was performed separately for each region. The GIS databases, including surface topography, underground geomaterial distribution, groundwater level, etc., for the GIS were established based on drilling data and monitoring data from 61 holes in the landslide area. A Visual Basic code was established to collect the results of Kriging from GIS and to prepare input data for limit equilibrium analysis (Chen, 2003).

3.2. Probability of failure

For slope engineering, probability of failure is generally considered as a simple index for risk evaluation. Although, theoretically and practically, the cost should be implemented to have the risk as probability of loss. Probability of failure can be defined as probability of safety factor less than 1.0 which can be obtained by integrating the probability density function for safety factor smaller than 1.0. We can define a performance function $G(X_i)$ for a slope as

$$G(X_i) = F(X_i) - 1 \quad (1)$$

where $F(X_i)$ is a function of safety factor. These two functions are all determined by input parameters X_i

($i=1$ to N) that can be considered as random variables. And the probability distribution of function $G(X_i)$ can be used to determine probability of failure for the slope it describes.

3.3. Monte Carlo analysis

Based on statistical sampling theory, Monte Carlo analysis is a very useful randomly simulation method, which can be applied by numerical computation. For a slope stability analysis, required parameters such as topography, groundwater level, failure mechanism, etc. can be found or assumed. But, other parameters such as mechanical properties and underground geology conditions are difficult to determine.

Considering the spatial uncertainty of those mechanical parameters, the Monte Carlo analysis randomly samples those parameters from their probability distributions, calculates a safety factor based on the chosen data set, and repeats the above sampling and safety factor calculation to obtain a series of safety factors. Though this process, we can obtain a probability distribution of safety factor.

For a slope of which stability is determined by control parameters X_i ($i=1$ to N), the safety factor Fs can be defined as function $Fs=F(X_\mathrm{i})$. Where X_i ($i=1$ to N) can be considered as random variables with probability distributions. By the Monte Carlo method, a set of X_i could be randomly sampled to determine a safety factor. Repeatedly performing the above process for $\boldsymbol{n}$ times; we can obtain n safety factors Fs_j ($j=1$ to n). If the number of safety factor less than one ($Fs \leqq 1$) is $\boldsymbol{m}$, then the probability of failure $\boldsymbol{P_f}$ is $\boldsymbol{m}/\boldsymbol{n}$.

For a large enough value of n, the probability density function of safety factor can be simulated. The probability of failure $\boldsymbol{P_f}$ can also be defined as

$$P_f = P(F_s \leq 1.0) \quad (2)$$

where $P(F_s \leq 1.0)$ denotes the probability of safety factor less than one. And $P(F_s \leq 1.0)$ can be determined by the ratio of the area under the distribution curve for safety factor less than 1.0 divided by the total area under the distribution curve.

In this study, according to data from literature review and laboratory tests, the probability density functions of cohesion and friction angle are considered as normal distributions. The mean value and standard deviation are 27.5° and 1.6° for friction angle, 2.95 t/m^2 and 0.26 t/m^2 for cohesion. Besides, based on literature review and monitoring data (NCHU, 2000; Su and Chen, 2002), the groundwater level is considered as exponential distribution with variance set to be 1.9 m.

3.4. Probabilistic stability analysis

In this study, the stability of a slope was evaluated by the limit equilibrium analysis, which consider the slope as if it were about to fail and determine the resulting shear stresses along the critical failure plane.

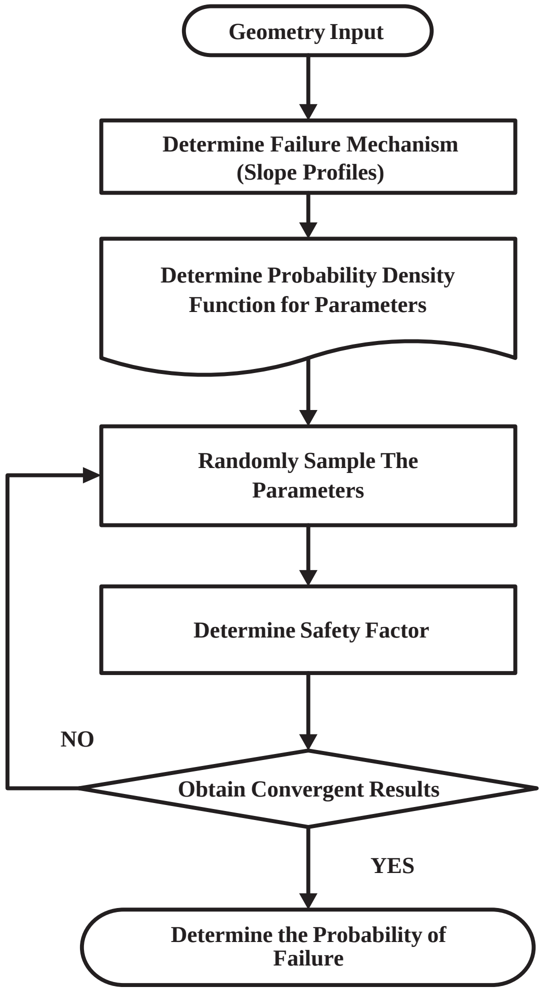

Fig. 6. Flowchart of the probabilistic risk analysis model.

Then, the safety factor can also determine as comparing these stresses with the shear strength:

$$F_s = \frac{\int s dl}{\int \tau dl} \quad (3)$$

where s is shear strength, τ is shear stress, and l is the length along the failure plane, and both integrals are calculated along its entire length.

The limit equilibrium analysis model PC-STABL6 (Bandini and Salgado, 1999) was adopted and applied in this study. PC-STABL6 features random techniques for generation of potential failure planes for subsequent determination of more critical planes and their corresponding safety factors. And the calculation of the safety factor against instability of a slope is performed by the method of slices. By the method of slices, the failure mass is divided into vertical slices such that integrations in Eq. (3) can be simplified for numerical calculation.

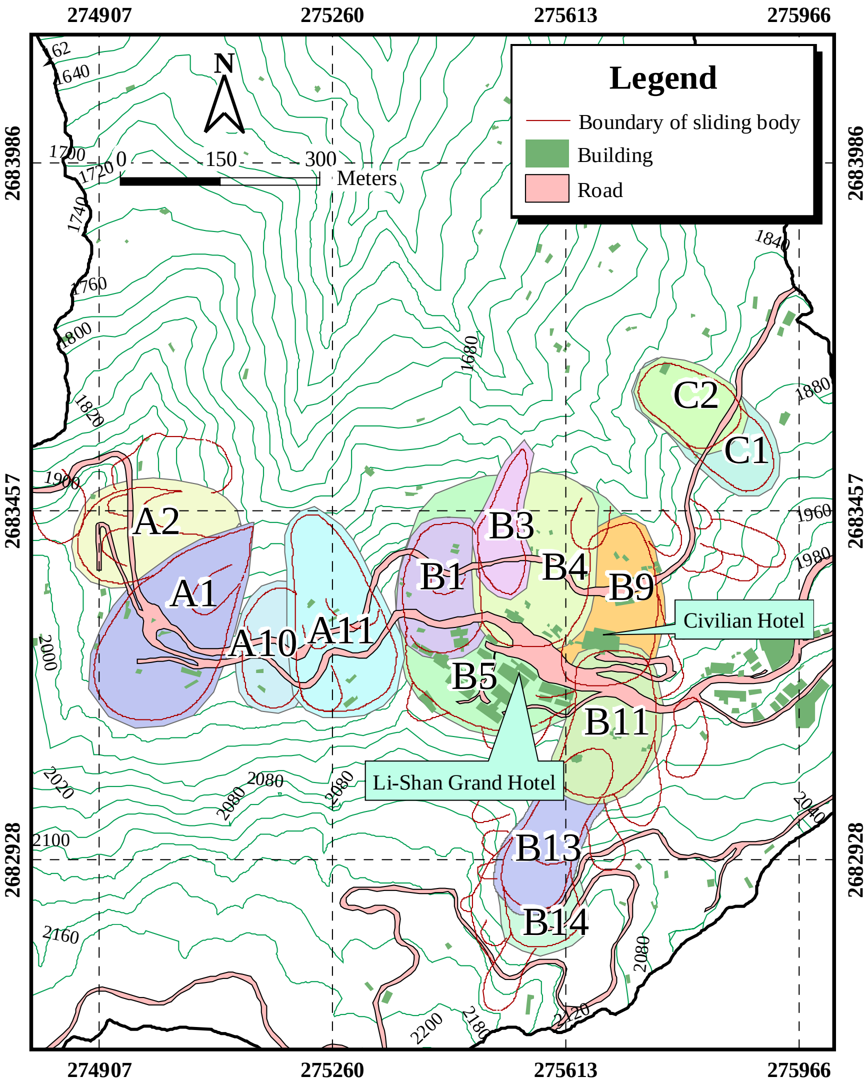

Fig. 7. Major sliding bodies for detailed analyses, sliding bodies A1, A2, A10 and A11 in the west region, sliding bodies B1, B3, B4, B5, B9, B11, B13, and B14 in the southeast region, and sliding bodies C1 and C2 in the northeast region.

To generate the potential failure planes, PC-STABL6 can employ a particular method, such as the simplified Bishop method (for circular shaped failure plane), the simplified Janbu method (for irregular shaped plane), etc. One special alternative provided is the sliding-block method, in which part of the sliding plane is piecewisely defined and the rest part is randomly chosen (Bandini and Salgado, 1999). In this study, the sliding-block method was adopted because the sliding planes can be partially defined according to tension crack and sliding plane obtained by field investigation or drilling.

For a sliding body, a segment of upper boundary and a segment of lower boundary are adopted; then, equally spaced 10 points can be found on each of those two segments. 100 testing profiles can be determined by connecting those boundary points and the three-dimensional elevation model obtained by GIS. With assumption of sliding planes, those geometry profiles can be used for two-dimensional limit equilibrium analysis. To consider the uncertainty of mechanical properties of geomaterial, input parameters are considered as random variables and determined by Monte Carlo sampling process. The flowchart of probability risk analysis can be shown in Fig. 6.

In this study, an interface for limit equilibrium analysis model PC-STABL6 was written in JAVA. Through this Window interface, a series of analyses can be easily performed to obtain the probability of failure for the slope analyzed. The Window interface comprises the following numerical steps: (1) importing data obtained by Monte Carlo sampling process, (2) assuming failure mechanism, (3) determining geomaterial profiles, (4) giving the total number of safety factor calculation, and (5) demonstrating the probability distribution of safety factor and find the probability of failure.

4. Results and discussion

The approach described in the previous section can be used to estimate the risk of slope failure. In this approach, beside the analysis profiles, input parameters are considered as random variables instead of single values. The risk evaluation problem is now deduced to determine the distribution of factor of safety. To calculate safety factors, the Monte Carlo technique, which randomly samples the input parameters from their probability distributions, is applied. For simplicity, generally for a complex simulation, input parameters are considered as independent variable; however, it is not always true in nature. From a preliminary sensitivity analysis, it suggests that the correlation of variables might not be significant in Lishan landslide area (Chen, 2003).

4.1. Influence of geomaterial and groundwater

For the sliding body B13 (see Fig. 7), through the probabilistic risk analysis, the most critical profiles can be found as shown in Table 3. As a sensitivity

Table 3
Ten most critical profiles of sliding body B13 for different conditions

Rank	Pre-remediation				Post-remediation					
	Parameter set 1		Parameter set 3		Parameter set 1		Parameter set 2		Parameter set 3	
	Profile	Safety factor	Profile	Safety factor	Profile	Safety factor	Profile	Safety factor	Profile	Safety factor
1	16	1.121	16	1.635	16	1.272	16	0.869	16	1.811
2	36	1.131	36	1.65	36	1.282	36	0.876	36	1.819
3	66	1.164	56	1.674	66	1.3	66	0.886	66	1.824
4	56	1.167	66	1.697	56	1.312	56	0.896	56	1.902
5	17	1.194	37	1.737	3	1.349	3	0.921	73	1.914
6	37	1.194	17	1.739	1	1.358	1	0.928	23	1.928
7	35	1.222	35	1.767	17	1.359	17	0.928	43	1.948
8	67	1.225	15	1.778	37	1.363	37	0.931	21	1.962
9	15	1.228	57	1.781	73	1.37	73	0.935	71	1.968
10	57	1.246	67	1.784	23	1.382	23	0.942	3	1.97

Parameter set 1: $C=3.0$ t/m2, $\varphi=28°$; parameter set 2 $C=2.0$ t/m2, $\varphi=20°$; parameter set 3 C=1.0 t/m2, $\varphi=40°$.

study, comparisons are made for different mechanical parameter sets as well as groundwater conditions. The pre-remediation groundwater surface is obtained by averaging the groundwater level during 1991–1992. And the post-remediation groundwater surface is assumed as the high groundwater level during 1997–1998. The major findings are:

1. In the pre-remediation phase, the rank of top 10 critical sliding profiles is the same if we adopt a different set of mechanical parameters (see Fig. 8).
2. For the same mechanical parameters, the most critical profile is still the same for pre-remediation and post-remediation phases. But, four of the top 10 critical sliding profiles are replaced (see Fig. 9). Therefore, the change of groundwater surface is critical for spatially estimating the risk.
3. From the comparison of results with the first data set and those with the third data set, it shows that three profiles (43, 21 and 71) in the top 10 critical profiles are replaced. On the other hand, the top 10 critical profiles are the same for the first data set and the second data set. It reveals that the spatial variation of risk is influenced by mechanical parameters only if they are significantly changed.

Besides, the most critical sliding profiles of sliding body B13 are mainly distributed in two lateral sides,

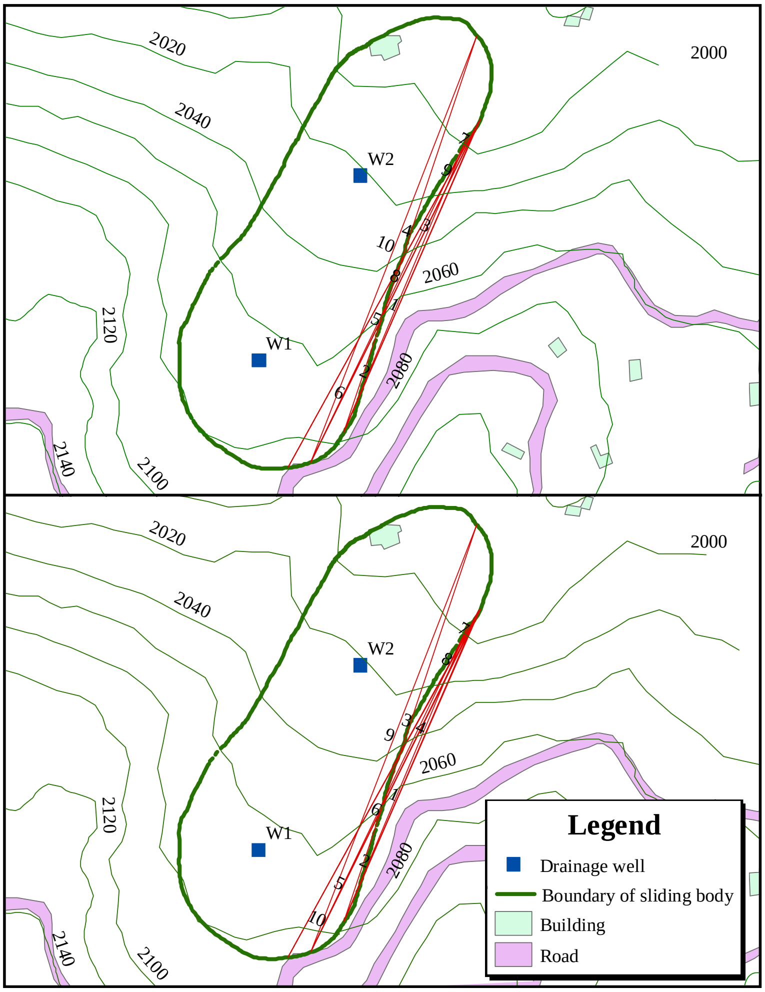

Fig. 8. Comparison of ten most critical profiles for sliding body B13 for different material property in pre-remediation phase. Top one is for parameter set 1 and bottom one is for parameter set 3.

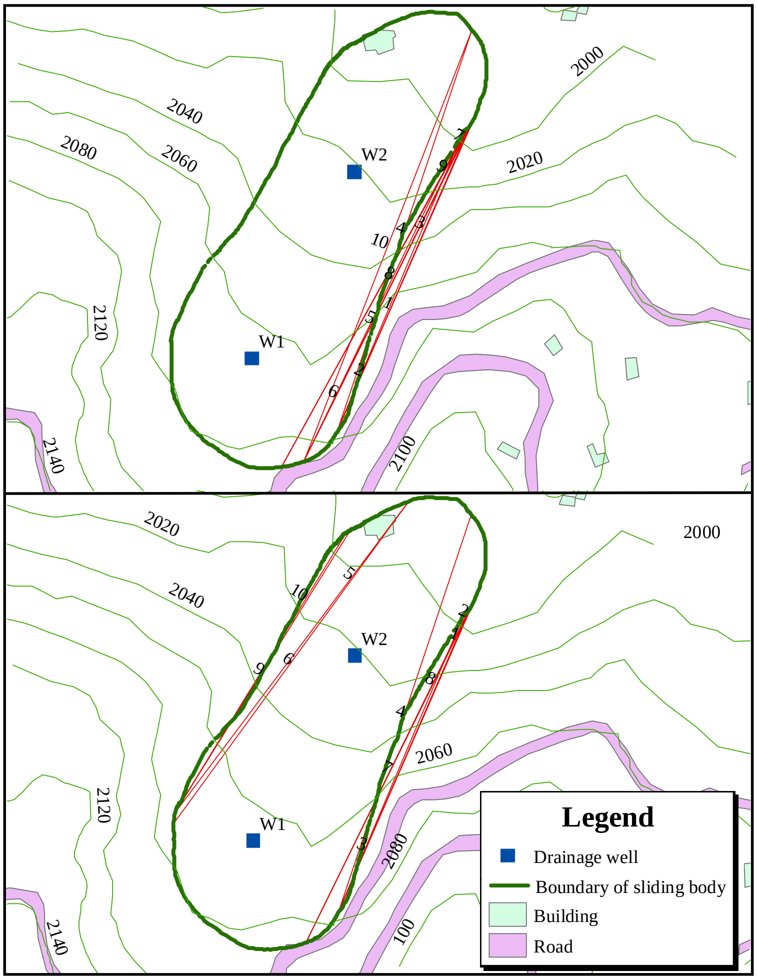

Fig. 9. Comparison of ten most critical profiles for sliding body B13 for material parameter set 1 in different phases. Top one is for pre-remediation phase and bottom one is for post-remediation phase.

as the sliding body B13 is located in the valley of a small stream. Therefore, topography is also an important control factor for the risk.

4.2. Risk evaluation

In this study, 14 major sliding bodies, i.e., sliding bodies A1, A2, A10 and A11 in the west region, sliding bodies B1, B3, B4, B5, B9, B11, B13, and B14 in the southeast region, and sliding bodies C1 and C2 in the northeast region, are adopted for detailed analyses (see Fig. 7). The risks of those sliding bodies are evaluated for different phases. Then the risk of a region can be considered as the mean of the major sliding bodies inside. And the major findings are:

4.2.1. Risk evaluation for different regions

Considering the groundwater surface before and after construction of drainage wells, it shows the risk changes from 59.42% to 99.97% for the west region, from 34.26% to 27.94% for the southeast region, and from 15.77% to 14.93% for the northeast region (see Fig. 10). The unreasonable results for the west region show the inaccuracy caused by poor quality and insufficient drilling data in this region. However, the lower risk for other regions reveals the performance of drainage wells.

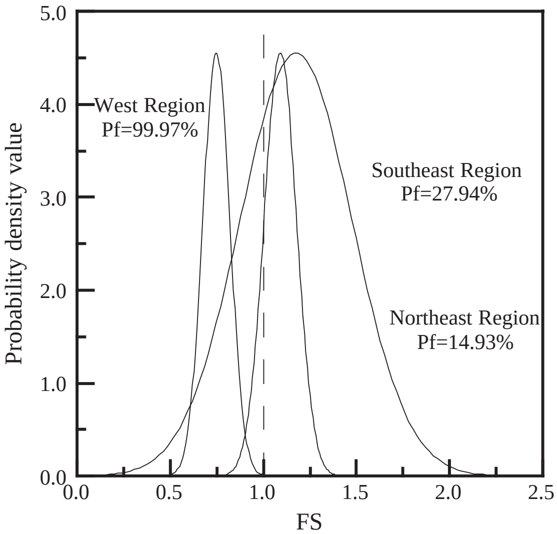

Fig. 10. Regional probability distributions of safety factor in post-remediation phase.

4.2.2. Risk evaluation for whole area

As the results of the west region are unreasonable due to not enough data, the risk of whole area is evaluated by excluding the four sliding bodies of the west region. For the risks of whole area before and after the construction of drainage wells, the risk reduces from 33.23% to 28.09% (as shown in Fig. 11). The results might reveal the effectiveness of the remediation.

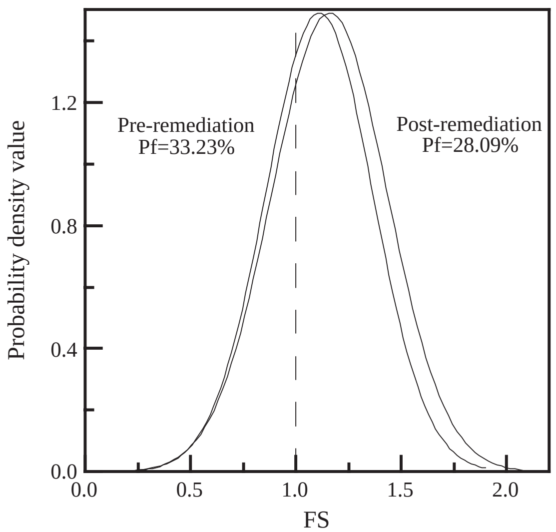

Fig. 11. Probability distributions of safety factor for whole area before and after remediation.

Table 4
Regional rank of risk for sliding bodies before and after remediation

Regional rank	Pre-remediation		Post-remediation	
	Sliding body	Mean value of safety factor	Sliding body	Mean value of safety factor
1	A11	0.979	A1	0.824
2	A10	1.022	A2	0.862
3	A1	1.203	A10	0.898
4	A2	1.227	A11	1.073
1	B3	0.797	B3	0.837
2	B4	0.912	B4	1.020
3	B5	1.054	B5	1.143
4	B9	1.070	B1	1.273
5	B1	1.163	B9	1.419
6	B13	1.260	B13	1.464
7	B11	1.941	B11	1.949
8	B14	2.018	B14	1.974
1	C2	1.093	C1	1.140
2	C1	1.113	C2	1.159

Another evidence for the performance of remediation could be the redistribution of risk in landslide area. The risks of sliding bodies for different phases are ranked and illustrated in Table 4 and Figs. 12 and 13. As the remediation components are mainly distributed in the center area of landslide area, more significant improvement of risk can be found in the center area. The risk of sliding bodies can also be regionally ranked to suggest the priority of further treatment (also see Table 4). It is worth-noting that more drillings in the west region are essential for risk estimation of better accuracy.

5. Conclusions and suggestions

Stability back analyses were employed to study the behavior of slopes in the Li-shan landslide. The slopes are quite stable for dry condition, but become critical for fully saturated condition. The remediation treatment is essential as the precipitation in this area is quite high.

In this study, coupling GIS with Monte Carlo analysis and limit equilibrium analysis, a probabilistic risk analysis method has been established for spatially analyze the risk of a landslide area. In order to more efficiently control the limit equilibrium analysis, an interface is also written in JAVA. The integrated

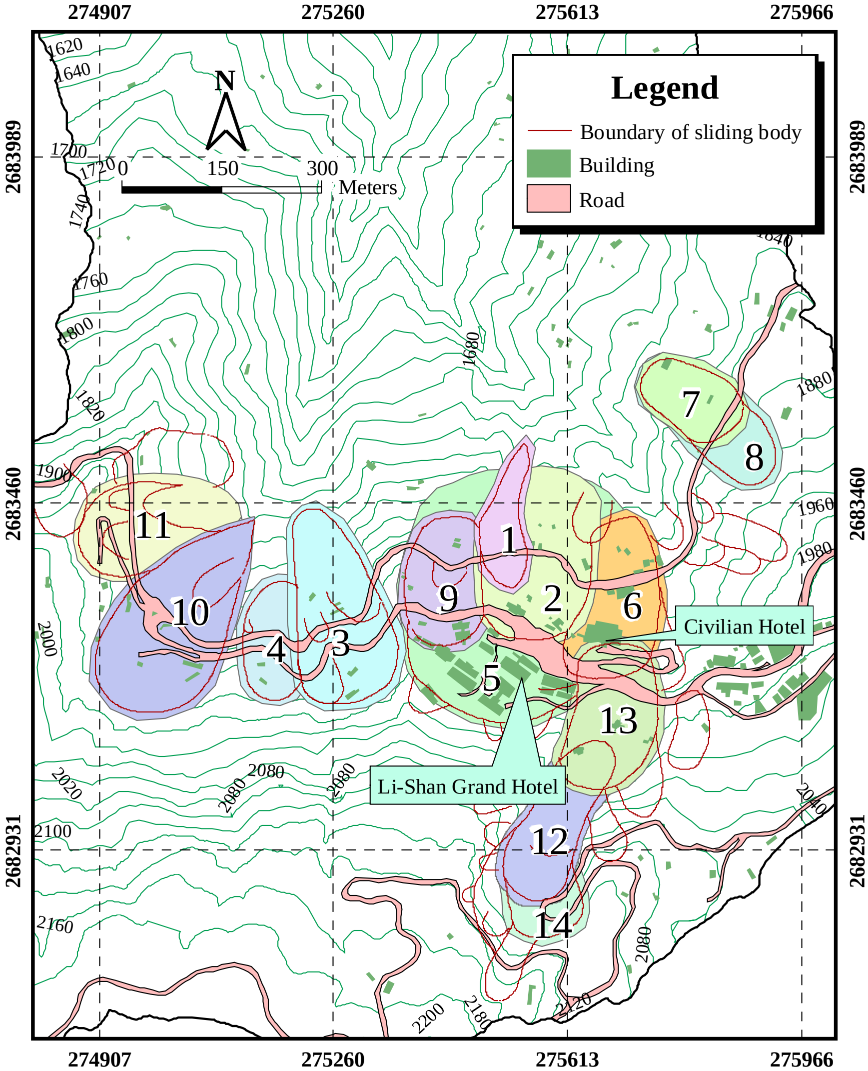

Fig. 12. Rank of risk for major sliding bodies in pre-remediation phase. The top 6 critical sliding bodies are concentrated in center area.

method was applied to estimate the risk of Li-shan landslide area.

Through a series of analyses, the risks of sliding bodies as well as sliding areas are evaluated. It shows the influence of groundwater level is significant, which reveals the importance of groundwater control and monitoring. The results also show that the safety of northeast area and southeast area are significantly improved as the groundwater levels are lowered by drainage wells. However, it is comparatively dangerous for the west area, which has been corroborated by further development of surface cracks.

The results show the improvement in terms of the change of probability is not so significant. This could be caused by different uncertainty levels of input variables or inter-dependency of the variables, which are essential issues for further development of the probabilistic analysis model. Other control factors, such as earthquake, heavy rain, and time effect are also important for practical risk estimation of a landslide. It will be worthy to consider those factors for further implementation. As drillings in the west and northeast areas are not sufficient, GIS cannot accurately obtain the three-dimensional ele-

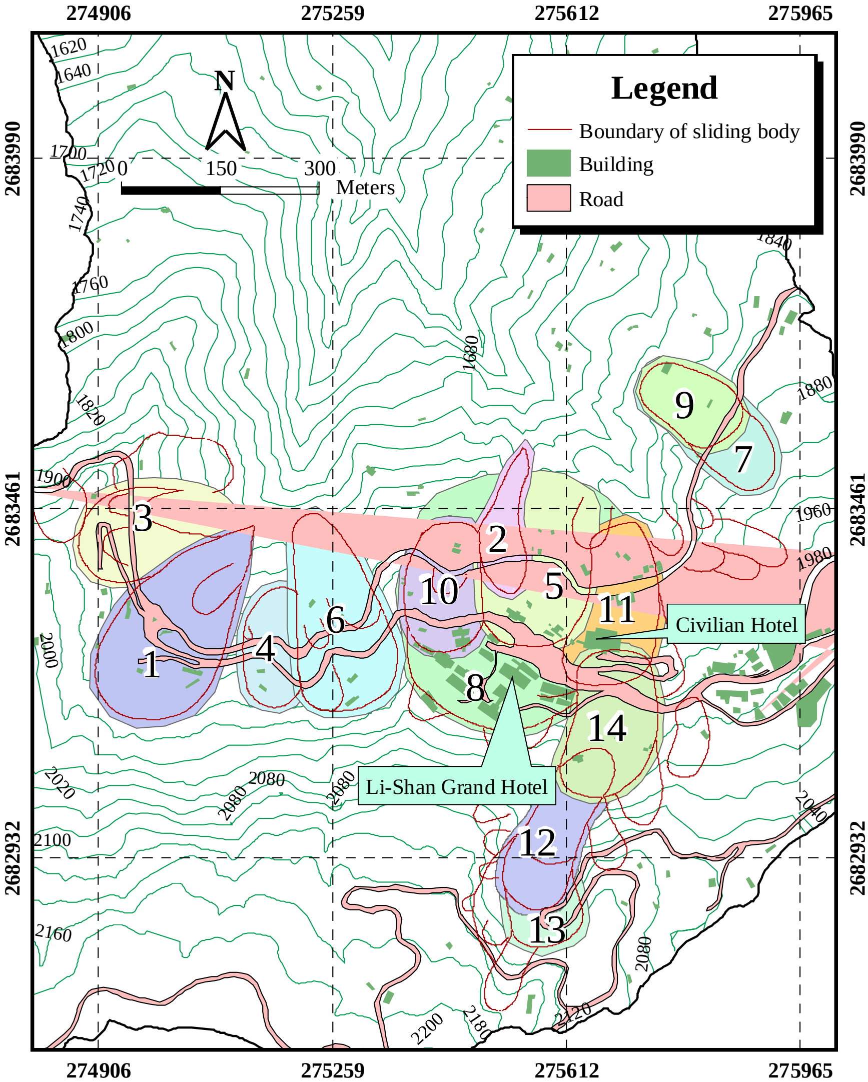

Fig. 13. Rank of risk for major sliding bodies in post-remediation phase. Risk has been dissipated from center area.

vation model. More drillings in those two areas are suggested.

Acknowledgements

The work presented in this paper was made possible through the support of the National Science Council and the Soil and Water Conservation Bureau, Taiwan, R.O.C. The authors are indebted to our colleague Prof. Miau-Bin Su and Dr. Y.H. Chen for their support. We also appreciate Prof. C.H. Juang and Dr. Th.W.J. van Asch for their critical reviews and constructive comments.

References

Bandini, P., Salgado, R., 1999. STABLE6 for DOS 6.0 User's Manual. Purdue University, U.S.

Chen, Y.L., 2003. Study on Risk Analysis of Slopes Considering Spatial Variability—A Case Study of Li-shan. Master thesis, NCHU, Taichung, Taiwan.

Chowdhury, R.N., 1982. Probabilistic risk analysis in geomechanics, water engineering. In: Chowdhury, R.N. (Ed.), Geomechanics, Water Engineering in Environmental Management. Balkema, Rotterdam (chapter 2).

Cressie, N., 1988. Spatial prediction and ordinary kriging. Mathematical Geology 20 (4), 405–421.

Energy and Resources Laboratories, ITRI, 1993. Planning on Investigation and Remediation for Li-shan Landslide, Final Report.

Ho, C.S., 1982. Tectonic evolution of Taiwan. Central Geological Survey, MOEA, Taiwan.

Hoek, E., 1994. The acceptable risks and practical decisions in rock engineering. Notes for Rock Mechanics Short Course, Taiwan, pp. 55–68.

Huang, C.S., 2002. Personal discussion on the incomplete geological map of Li-shan, 1:50000. Central Geological Survey, MOEA, Taiwan.

Jibson, R.W., Harp, E.L., Michael, J.A., 1999. A Modeling Procedure to Produce Probabilistic Seismic Landslide Hazard Maps, Abstracts with Programs, Geological Society of America, 1999 Annual Meeting, vol. 31(7), p. 195.

Juang, C.H., Jhi, Y.Y., Lee, D.H., 1998. Stability analysis of existing slopes considering uncertainty. Engineering Geology 49, 111–122.

Khazai, B., Sistar, N., 2000. Assessment of seismic slope stability using GIS modeling. Geographic Information Sciences 5 (2), 121–128.

Lu, C.Y., Chu, H.T., Lee, J.C., Chan, Y.C., Chang, K.J., 2000. Impact of basement high on the structure and kinematics of western Taiwan thrust wedge-example from 1999 Chi-Chi Taiwan earthquakes. Int. Workshop on Annual Commemoration of Chi-Chi Earthquake, Taipei, pp. 145–154.

National Chung-Hsing University, 2000. Establishment and application of databases for Li-shan landslide, monitoring data section. Report to the Soil and Water Conservation Bureau, Taiwan.

Nguyen, V.U., 1985. Safety factors and limit states analysis in geotechnical engineering. Canadian Geotechnical Journal 22, 144.

Pack, R.T., Tarboton, D.G., Goodwin, C.N., 1998. The SINMAP approach to terrain stability mapping. 8th Congress of the IAEG, Vancouver, Canada.

Shou, K.J., 2002. Geology in Li-shan area. Workshop on Performance Evaluation of Li-shan Landslide Remediation, Taichung, Taiwan, pp. 121–142 (in Chinese).

Shou, K.J., Su, M.B., 2002. On the failure mechanism and remediation of the Li-shan landslide in Taiwan. Int. Conf. Mountain Environment and Development, Chengdu.

Shou, K.J., Wang, C.F., 2003. Analysis of the Chiufengershan landslide triggered by the 1999 Chi-Chi earthquake in Taiwan. Engineering Geology 68, 237–250.

Su, M.B., Chen, D.T., 2002. Monitoring system and databases. Workshop on Performance Evaluation of Li-shan Landslide Remediation, Taichung, Taiwan, pp. 121–142 (in Chinese).

Zhou, G., Esaki, T., Mitani, Y., Xie, M., Mori, J., 2003. Spatial probabilistic modeling of slope failure using an integrated GIS Monte Carlo simulation approach. Engineering Geology 68, 373–386.